Continuous Phase-Shifted Selective Harmonic Elimination and DC-Link Voltage Balance Solution for H-bridge Multilevel Configurations, Applied to 5L HNPC

Alain Sanchez-Ruiz, *Member, IEEE*, Gonzalo Abad, *Member, IEEE*, Ivan Echeverria, Iñigo Torre, and Iñigo Atutxa

***Abstract*—This paper proposes a method for calculating selective harmonic elimination (SHE) angle solutions applied to multilevel voltage waveforms (of more than three levels of voltage): Phase-shifted SHE (PS-SHE). This technique is based on the calculation of simple SHE angles, increasing the number of levels and minimized harmonics by means of phase shift application. Compared to classical calculation, continuous SHE solution can be achieved for the whole modulation index range. Added to this, dc-link voltages balancing strategy is proposed for converters based on single-phase H-bridge (HB) configurations with multilevel (more than two levels) arms, using SHE. It is based on a prediction of the neutral point current and a hysteresis band. This strategy does not increase the number of commutations and shares them equally among the arms inside the HB. The good performance of the two proposed techniques (PS-SHE and dc-link neutral point regulation strategy) are proven into a downscaled five-level HB neutral-point-clamped (5L HNPC) converter topology. The carried out tests prove the suitability of the proposed techniques.**

***Index Terms*—DC-link voltage control, five-level H-bridge (HB) neutral-point clamped (5L HNPC), HB, modulation, neutral point clamped (NPC), selective harmonic elimination (SHE), single phase, voltage source converters (VSCs).**

I. Introduction

MULTILEVEL voltage source converters (VSCs) are a mature technology. Their importance is exponentially increasing as applications demand higher power and waveform quality [1]. The usage of this type of power electronic equipment has spread more and more as harder working conditions and operating standards to fulfill are required. In fact, multilevel converters are now being used for different and varied applications such as:

1) drives [2]–[4]. Several drives applications can be found in: industry, electric vehicles, railway, ship propelling, etc. Main characteristic is the output variable frequency;
2) grid oriented [5]–[7]. This type of applications are renewable energies integration, power transmission, grid codes fulfillment, etc. As main characteristic, working for the grid side, constant output frequency can be highlighted.

In many applications as higher power rate as possible is demanded to the converter. Additionally, though output waveform quality standards are also asked. These two requirements make it important to optimize the switching pattern of the converter. Moreover, reducing the number of commutations may increase the output available current, or can give the option of increasing the output frequency of the converter (for high-speed drives) [8].

The orders to the power semiconductors are commonly given by means of modulation techniques [4]. Several modulation techniques are known for high-power applications. While sinusoidal pulsewidth modulation (PWM [9], [10]) is focused on its implementation simplicity, space vector modulation (SVM [11]) has more controllability. However, when the number of commutations needs to be minimized, selective harmonic elimination (SHE [12]–[14]) techniques present a clear advantage for this purpose. SHE employs off-line switching angles calculations with the aim of eliminating undesired harmonic content in the output voltage spectrum. Many variants have been proposed derived from SHE, such as selective harmonic minimization/mitigation (SHM [15]), synchronous optimal PWM [16], etc.

Therefore, in a multilevel converter, two main tasks need be performed.

1) Reference voltage synthesizing. In SHE, the synthesized voltage is directly dependent on the calculated angles. In fact, the more levels the voltage has and the bigger the number of employed angles is, the difficulty of the off-line calculation becomes bigger [12]–[14], [17], [18]. This may lead to discontinuous angle set solutions for SHE of more than three levels. Thus, this discontinuity may provoke current peaks if a proper transition is not executed.
2) DC-link capacitors voltage balancing. Using SHE this task is not straightforward. Most of the literature methods increase the number of commutations or move the switching angles [12], [19]–[23]. Therefore, power losses will be increased (which is the opposite of what is wanted with SHE solutions) or a proper elimination of harmonics will not be achieved, respectively.

Both, calculating optimal SHE angles and achieving a good dc-link voltage balance interaction are necessary to optimize the overall converter performance.

Manuscript received September 23, 2014; revised April 11, 2016; accepted May 16, 2016. Date of publication June 1, 2016; date of current version January 20, 2017. Recommended for publication by Associate Editor B. Lehman.

A. Sanchez-Ruiz, I. Echeverria, I. Torre, and I. Atutxa are with Ingeteam Power Technology S.A., 48170 Zamudio, Spain (e-mail: alain.sanchez@ingeteam.com; ivan.echeverria@ingeteam.com; inigo.torre@ingeteam.com; inigo.atutxa@ingeteam.com).

G. Abad is with the Electronics and Computing Department, University of Mondragon, Mondragon 20500, Spain (e-mail: gabad@mondragon.edu).

Color versions of one or more of the figures in this paper are available online at http://ieeexplore.ieee.org.

Digital Object Identifier 10.1109/TPEL.2016.2574931

Among the commercialized multilevel converter topologies, many are employed for medium-voltage and high-power applications [4]. One of the alternatives to increase the output voltage is the use of H-bridge (HB) solutions with multilevel branches. One of these topologies is the five-level HB neutral-point-clamped (5L HNPC) topology [3], [8], [16], [23]–[26]. This topology is formed by the H connection of two 3L NPC branches, linking each HB within star configuration.

This paper is focused on the calculation of multilevel SHE and its dc-link neutral point control oriented to 5L HNPC converter topology. A novel method to calculate multilevel SHE angles is presented, called the phase-shifted SHE (PS-SHE), which reduces the SHE calculation complexity and then applies some minimization techniques to increase the number of levels. Thanks to this calculation simplification, continuous SHE angles throughout a big modulation index gap are achieved, which is not achieved in the literature. This method can be applied to calculate angles for any converter topology.

Added to this, a dc-link voltage balancing algorithm is proposed, oriented to HB converter topologies with multilevel branches; in this case this is applied to a 5L HNPC. The dc-link voltage balancing strategy is based on the neutral point current prediction and a hysteresis band, taking advantage of the redundant vectors the HB topologies have, without increasing the number of commutations.

The paper starts with SHE formulation problem explanation and serving the proposal of the novel PS-SHE. Next, a dc-link balancing algorithm for HB configuration converters is proposed, focusing on 5L HNPC. The paper concludes with experimental results of PS-SHE technique and neutral point control, demonstrating the suitability of the solution.

II. Phase-Shifted SHE

A. Mathematical Formulation of SHE

SHE mathematical formulation depends on the number of levels of the voltage that is wanted to be calculated. Fig. 1 presents different SHE alternatives depending on the number of levels of the output voltage. The generic modulation index (from 0 to 1, where 1 means square wave modulation) formulation used in this paper is

$$m_a = \frac{\pi}{(L-1)\cdot\sqrt{2}} \cdot \frac{V_{1,\mathrm{rms}}}{E} \tag{1}$$

where L is the number of levels of the converter simple voltage, $V_{1,\mathrm{rms}}$ refers to the root-mean-square (rms) value of the converter fundamental simple voltage, and E is the voltage step of the output voltage for a known topology. Added to this, converter SHE switching angles will be named as

$$0 < \alpha_1 < \alpha_2 < \cdots < \alpha_N < \frac{\pi}{2} \tag{2}$$

where N is the number of calculated angles in the first quadrant. Once the first quadrant is calculated, symmetry is applied to complete the whole fundamental period.

Fig. 1 shows SHE calculating examples in the case of three and five output levels, respectively. In this figure, V_{R0} represents the simple converter voltage (from one output terminal to the dc-link neutral point in three-phase systems; HB terminals voltage in single-phase configurations).

As it can be concluded from Fig. 1, two different cases can be distinguished when calculating SHE angle families.

1) If a three-level waveform is analyzed (Fig. 1(a) and (3)), voltage levels go from E to 0 if the voltage reference is positive, and from 0 to $-E$ if it is negative. Thanks to the symmetry of the positive and negative semiperiods, even harmonics are ideally eliminated. Due to this reason, they do not need to be eliminated, using SHE angles to control/eliminate odd harmonics which are not multiple of 3.
2) When the number of voltage levels is higher than four (see Fig. 1(b) and (4), henceforth called multilevel SHE, ML-SHE), the equations to be solved change. For instance, considering a five-level waveform, voltage levels can go from 0, E and $2E$ values if the voltage reference is positive, while they can take 0, $-E$, and $-2E$ values if voltage reference is negative. As it happens with three-level waveforms, applying symmetry in positive and negative semiperiods, even harmonics are eliminated. In this way, only odd harmonics which are not multiple of 3 need to be controlled/eliminated.

If Fig. 1(a) and (b) are compared, a main difference can be seen: while in 3L SHE the voltage goes from 0 to E and viceversa; when 5L SHE voltage is in E, a voltage step (E) can be increased or decreased. If actual voltage is E, next voltage level can be 0 or $2E$. This does not happen in 3 level waveform. Due to this fact, the cosines have a "$\pm$" sign in (4); while in (3) voltage transition is completely known "$(-1)^{k+1}$". This fact increases exponentially the number of cases of the equations to be solved in ML-SHE (4).

Many studies have tackled the task of solving ML-SHE equations in literature [12]–[14], [17], [18], [27]–[30]. However, all the references achieve discontinuous angles along the modulation index (m_a).

For instance, Fig. 2 shows the obtained angle solutions for a five-level SHE, solving ML-SHE (4). In order to solve these equations MATLAB software is used. Top plot shows the SHE angles, while the bottom plot shows a "-1" when in a calculated angle a voltage step needs to be subtracted and a "$+1$" when in a calculated angle a voltage step needs to be added. In this example, 6 calculated angles are employed. One of the angles is employed to control the fundamental voltage. Each of the remaining five angles do eliminate one undesired harmonic, achieving the elimination of 5th, 7th, 11th, 13th, and 17th harmonics. The first appearing harmonic in line-to-line voltage would be the 19th. However, discontinuous angle solutions are attained along the whole modulation index range. This transition from one angle gap to another may provoke the necessity of complex algorithms to change from one angle set to another (big switching angles difference and switching sign change); thus, undesired current peaks in the load may appear.

If Fig. 2 is analyzed, different angle sets can be identified along the whole modulation index range. However, not all of them do perform a voltage pattern change. This can be noticed

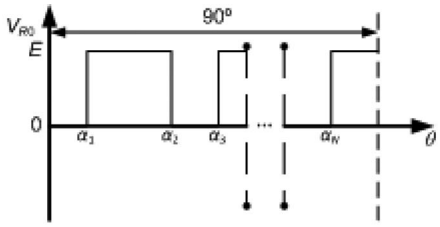

(a)

$$\sum_{k=1}^{N}(-1)^{k+1}\cdot\cos(\alpha_k)=m_a$$
$$\sum_{k=1}^{N}(-1)^{k+1}\cdot\cos(n\cdot\alpha_k)=0,\quad n=5,7,11,13\ldots \tag{3}$$

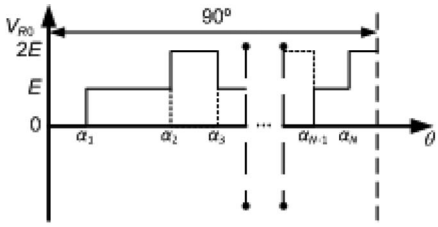

(b)

$$\sum_{k=1}^{N}\pm\cos(\alpha_k)=m_a$$
$$\sum_{k=1}^{N}\pm\cos(n\cdot\alpha_k)=0,\quad n=5,7,11,13\ldots \tag{4}$$

Fig. 1. SHE formulation. (a) 3L SHE. (b) 5L SHE.

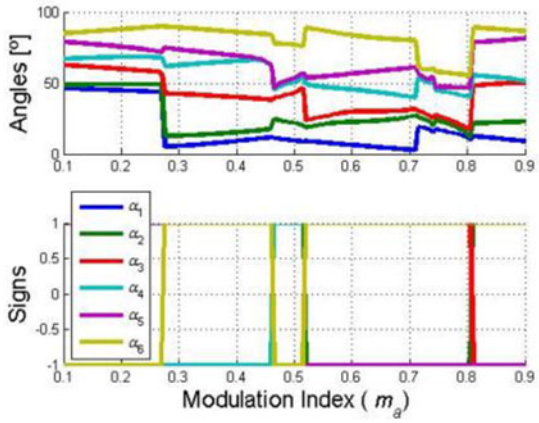

Fig. 2. 5L ML-SHE6 solution for five-level output waveform and six calculated angles using (4). Angles represent the switching angles of the first quadrant for different modulation indices. Signs represent whether the each switching is positive (add a step) or negative (subtract a step).

looking to the sings of the transitions of the switching angles (whether a voltage step is added or subtracted). Hence, this transitions from angle sets with different voltage patterns are the most problematic, from the point of view of transition algorithms. Added to this, the charges injected/extracted from the neutral point have a big variation from one modulation index to other, making the dc-link behavior more unstable.

B. Proposed Calculation: PS-SHE

Thecomplexity of solving ML-SHE (4) is clear. Hence, the approach proposed in this paper to address this problem is PS-SHE. This proposal is based on calculating SHE angle sets for a number of levels where equations to be solved have three levels (3), being easier to converge to a solution. Afterwards, recursive phase shifts are proposed to be applied to the original SHE angles. Thus, minimization of harmonics is attained, while the level of voltages and number of calculated angles are increased in the same time. As original equations in (3) are simpler, continuous angle solution is achieved for the whole modulation index range.

TABLE I
HARMONICS BEHAVIOR WHEN APPLYING DIFFERENT β ANGLES [31]

n	r_n			
	$\beta=15°$ ($n_{\text{elim}}=6$)	$\beta=7.5°$ ($n_{\text{elim}}=12$)	$\beta=5°$ ($n_{\text{elim}}=18$)	$\beta=3.75°$ ($n_{\text{elim}}=24$)
1	1.9319	1.9829	1.9924	1.9957
5	0.51764	1.5867	1.8126	1.8939
7	−0.51764	1.2175	1.6383	1.7937
11	−1.9319	0.26105	1.1472	1.5037
13	−1.9319	−0.26105	0.84524	1.3187
17	−0.51764	−1.2175	0.17431	0.88458
19	0.51764	−1.5867	−0.17431	0.64288
23	1.9319	−1.9829	−0.84524	0.13081
25	1.9319	−1.9829	−1.1472	−0.13081
29	0.51764	−1.5867	−1.6383	−0.64288
31	−0.51764	−1.2175	−1.8126	−0.88458
35	−1.9319	−0.26105	−1.9924	−1.3187
37	−1.9319	0.26105	−1.9924	−1.5037
41	−0.51764	1.2175	−1.8126	−1.7937
43	0.51764	1.5867	−1.6383	−1.8939
47	1.9319	1.9829	−1.1472	−1.9957
49	1.9319	1.9829	−0.84524	−1.9957

An example of how a phase shift is done is shown in Fig. 3. In this example, V_{in} represents a generic waveform of the first 90º of 3L SHE3 (3 level SHE of 3 calculated angles); these angles are calculated using (3). The main idea is minimizing all the harmonics that the original 3L SHE has not eliminated.

If one v_{in} waveform is phase shifted with β angle ($v_{\text{in},\beta}$), another one with $-\beta(v_{\text{in},-\beta})$ and both are added, resultant waveform is v_{out}. Each of the harmonics (including the fundamental) of the resultant waveform can be calculated by means of

$$\begin{aligned} &v_{n,\text{in}}\cdot(\cos(n\beta)+j\sin(n\beta))\\ &\quad+v_{n,\text{in}}\cdot(\cos(n\beta)-j\sin(n\beta))\\ &\quad=2\cdot v_{n,\text{in}}\cdot\cos(n\beta)=r_n\cdot v_{n,\text{in}}=v_{n,\text{out}} \end{aligned} \tag{5}$$

where $v_{n,\text{in}}$ is the *n*-order harmonic voltage value of the original 3L SHE angles, $v_{n,\text{out}}$ is the *n*-order harmonic voltage value of the addition of two phase shifted waveforms, and r_n is the ratio between the *n*-order 3L SHE input harmonic and the output

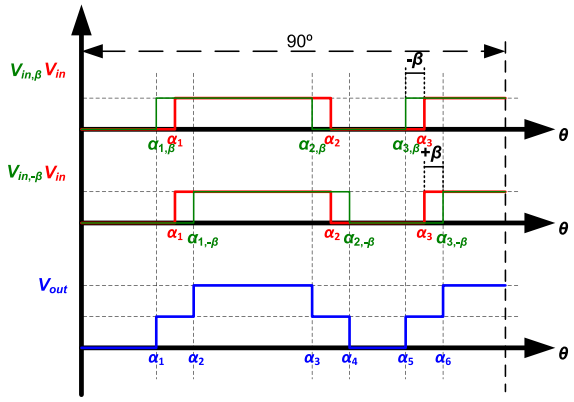

Fig. 3. Evolution of input 3L SHE waveforms (v_{in} in red), the input phase shifted waveforms ($v_{\text{in},\beta}$ and $v_{\text{in},-\beta}$ in green) and the output ones ($v_{\text{out}} = v_{\text{in},\beta} + v_{\text{in},-\beta}$ in blue).

one. It can go from 0 to 2. Some examples of different β phase shifts and resultant r_n ratios for different harmonics are given in Table I.

Ideally, if $\beta = 0$, the original v_{in} waveform harmonics would be doubled in v_{out}. However, applying $\beta \neq 0$, fundamental harmonic is reduced, but a minimization of some other harmonics is attained (highlighted in Table I, values smaller than "1" represent that a minimization has occurred).

The β angle choice depends on the first harmonic group that appears in the original SHE waveform, which marks the first harmonics that need to be mitigated

$$\cos\left(n_{\text{elim}} \cdot \beta\right) = 0 \rightarrow \beta = \frac{90}{n_{\text{elim}}} \tag{6}$$

where n_{elim} is the harmonic to be eliminated. If n_{elim} harmonic is eliminated, $(n_{\text{elim}} \pm 1)$ are directly mitigated. Therefore, if a pair of harmonics is wanted to be mitigated, the harmonic number in the middle of the one it is needed to be eliminated. For instance, in order to mitigate 5th and 7th harmonics, $n_{\text{elim}} = 6$ needs to be selected in (6). Furthermore, the minimization (n_{minim} represents the minimized harmonics) inherently is repeated in higher harmonics

$$n_{\text{minim}} = (2 \cdot k - 1) \cdot n_{\text{elim}} \pm 1 \tag{7}$$

where k is an integer number ($k = \{1, 2 \ldots\}$), as it can be seen in Table I.

This phase shift can be used as many times as wanted when constructing a waveform of higher number of levels. In each minimization stage, different pair of harmonics can be minimized. Thus, more levels are gained and more harmonics are minimized each time the phase shift is applied. The number of switching angles of the resultant waveform are doubled too. On the contrary the maximum achievable voltage will decrease. Furthermore, as phase shift is applied, depending on how many phase shifts are applied, the number of calculated angles per output levels is limited. Table II illustrates the possible number of angles depending on desired resultant output voltage waveform levels. In this table, N_{3L} represents the number of calculated angles in the 3L SHE, calculated using (3). While $L = 3$ means using the original 3L SHE angles, $L = 5$ means applying one phase shift, $L = 9$ means applying two phase shifts, etc.

TABLE II
RESULTANT NUMBER OF ANGLES OF THE FINAL WAVEFORM, DEPENDING ON THE INITIAL NUMBER OF ANGLES AND DESIRED NUMBER OF LEVELS

	$N_{3L} = 1$	$N_{3L} = 2$	$N_{3L} = 3$	$N_{3L} = 4$	$N_{3L} = 5$
$L = 3$	1	2	3	4	5
$L = 5$	2	4	6	8	10
$L = 9$	4	8	12	16	20
$L = 17$	8	16	24	32	40
$L = 33$	16	32	48	64	80

As it can be deducted, when the calculated waveform has more than three levels, the resultant angles can go out of the first quadrant. If applying the phase shift some angles overpass the 90º they are brought back to the first 90º

$$\alpha_{k,\text{out}}\ (m_a) = 180 - \alpha_{k,\text{in}}\,(m_a)\,. \tag{8}$$

On the contrary, if after β phase shift injection the resultant angle goes below zero, the equation presented is applied

$$\alpha_{k,\text{out}}\ (m_a) = -\alpha_{k,\text{in}}\,(m_a)\,, \tag{9}$$

where $\alpha_{k,\text{in}}$ represents one of the angles after applying the β phase shift (lower plot in Fig. 4(a)), and $\alpha_{k,\text{out}}$ names the final angles after bringing them to the first operating quadrant. When one angle is brought to the first quadrant, its commutation sign needs to be swapped.

The upper plot of Fig. 4(a) shows the calculation of 3L SHE3 applying (3). These angles control the fundamental harmonic's amplitude and eliminate the 5th and the 7th. Next, the lower plot of Fig. 4(b) shows the original 3L SHE3 angles with $\pm\beta = 7.5^{\circ}$ phase shift; thanks to this, 11th and 13th harmonics are minimized in 5L angles. As it can be observed, some of the phase shifted angles exceed the 0º−90º limits. After applying the transformations proposed in (8) and (9), final achieved angles for 5L PS-SHE6 are illustrated in Fig. 4(b). Accordingly, in this Fig. 4(b) switching angles of the 5L waveform can be seen, together with the switching signs of each angle (whether a voltage step is added or subtracted).

Same strategy is followed in order to calculate Fig. 4(c), the original 3L SHE1 angles (controlling the fundamental harmonic) are achieved using (3). Then, thanks to the phase shift, 5L PS-SHE2 is achieved, which also achieves the minimization of 5th and 7th harmonics.

For instance, as a matter of summarizing it, achieved 5L ML-SHE6 (calculated using (4), Fig. 2) and 5L PS-SHE6 (calculated using (3), Fig. 4(b)) are listed as follows:

1) 5L ML-SHE6 controls 1st harmonic and eliminates 5th, 7th, 11th, 13th, and 17th harmonics;
2) 5L PS-SHE6 controls 1st harmonic, eliminates 5th and 7th, and minimizes 11th and 13th (and higher harmonics as (7)).

However, a whole modulation index continuous solution can be achieved using PS-SHE. This continuity can be important enough to let the converter have worse total harmonic distortion

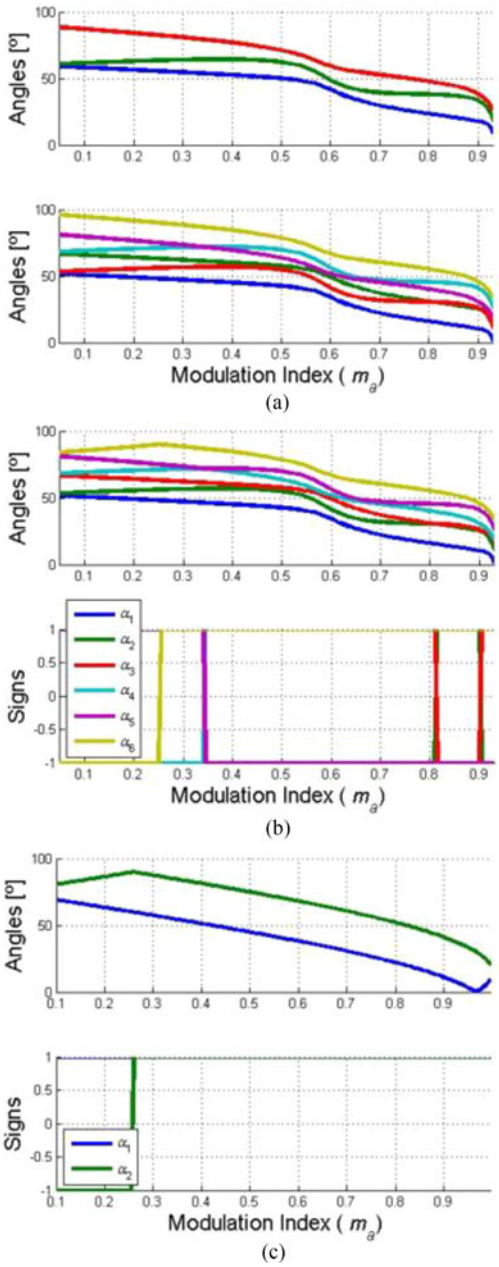

Fig. 4. 5L PS-SHE angle solutions. (a) PS-SHE6 angles definition with three switching angles to six switching angles thanks to β injection. (b) Angles and signs for PS-SHE6, minimizing 11th and 13th harmonics. (c) Angles and signs for PS-SHE2, minimizing 5th and 7th harmonics.

(THD), which, especially in motor-oriented inverters, can be considered quite attractive.

III. DC-Link Capacitors Voltage Balancing Using SHE for HB Multilevel Configurations

This section proposes a novel dc-link capacitors voltage balancing strategy for SHE modulation, which can be applied to HB multilevel converter topologies, with multilevel branches. Thanks to the redundancies in HB configurations with multilevel branches, this method predicts the dc-links voltages behavior, accomplishing a proper capacitors voltages balancing. This is

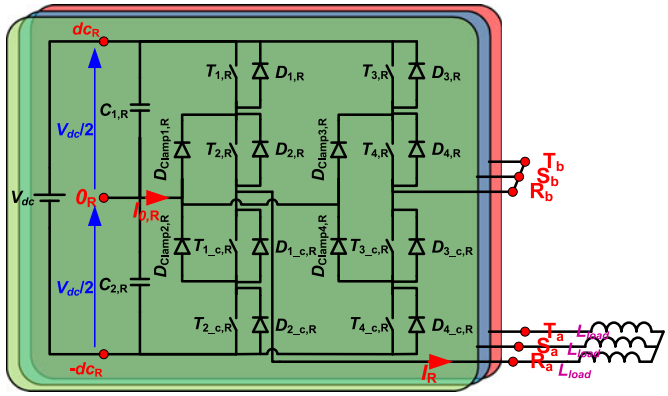

Fig. 5. Three-phase 5L HNPC converter scheme.

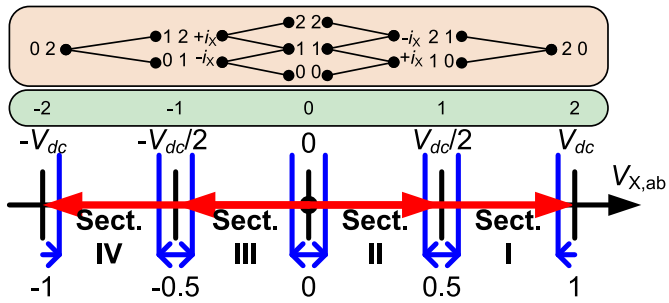

Fig. 6. Space vector for one HB. $V_{\mathrm{X,ab}}$ is the terminals voltage in X phase.

carried out using a hysteresis band, with no extra commutation. This strategy is applied into a 5L HNPC three-phase converter configuration [3], [8].

A. 5L HNPC Topology

The 5L HNPC is a widely spread converter topology, specially focused on Medium Voltage (MV) applications [4]. Each HB is constructed by means of two 3L NPC branches, achieving five-levels in the HB output terminals. This scheme is repeated three times in order to have one HB per output phase. One output terminal of each HB is linked in star connection. $(\mathrm{R_b}, \mathrm{S_b}, \mathrm{T_b})$. On the other hand, the other three terminals are directly connected to the load $(\mathrm{R_a}, \mathrm{S_a}, \mathrm{T_a})$. The scheme is shown in Fig. 5. Each HB needs compulsorily to be fed by isolated dc sources, normally fed by a multipulse transformer and diode front ends for a drive application.

Each HB is able to attain five different voltage levels between its terminals (v_H), which are accomplished by means of nine different switches states (inside the HB, v_{SW}). Fig. 6 shows the space vector for each HB, which is modulated independently. In order to define the switching states within the HB two numbers are used; each of which corresponds to the voltage value of each branch of the HB, where 0 is 0 V with respect to the neutral point of the dc-link, 1 is $V_{\mathrm{dc}}/2$ and 2 is V_{dc}. On the contrary, the HB output voltage is represented by a number, which is the subtraction of both branches. A brief summary of possible HB states can be seen in Table III. In this table too,

TABLE III
5L HNPC VECTORS SUMMARY (IN RED, STATES NOT USED WITH SHE)

$V_{X,ab}$	V_H	V_{SW}		T_1	T_2	T_3	T_4	$I_{0,X}$
		$V_{SW,a}$	$V_{SW,b}$					
V_{dc}	2	2	0	1	1	0	0	-
$V_{dc}/2$	1	2	1	1	1	0	1	$-I_X$
		1	0	0	1	0	0	$+I_X$
0	0	2	2	1	1	1	1	-
		1	1	0	1	0	1	
		0	0	0	0	0	0	
$-V_{dc}/2$	-1	1	2	0	1	1	1	$+I_X$
		0	1	0	0	0	1	$-I_X$
$-V_{dc}$	-2	0	2	0	0	1	1	-

how the neutral point depends on the load current is given, where $\mathrm{X} = \{\mathrm{R}, \mathrm{S}, \mathrm{T}\}$. Furthermore, $T_{1,4}$ represent the gate orders of the transistors noted in the same way as in Fig. 5; the "_c" in the same of the transistors means that they are complementary.

As Table III shows, $V_{\mathrm{dc}}/2$ and $-V_{\mathrm{dc}}/2$ voltages present two ways to be synthetized inside the HB. They are called redundant vectors. Each of these semiconductor paths, injects the output phase current in same magnitude but opposite sign into the dc-link neutral point. Each time these output voltages are synthesized, the neutral point voltage of the HB is altered. The redundant vectors usage is one of the bases of the proposed dc-link neutral point balancing algorithm in the following points.

Furthermore, if Table III is analyzed, in order to synthesize 0V in the HB terminals, three different switching combinations can be applied: 00, 11 and 22. However, the use of 00 and 22 is discarded, since 11 does not add any extra commutation when a transition to the closer voltage levels (21, 10, 01, 12) is done. Due to this reason, 00 and 22 are marked in bold in Table III.

B. SHE Applied to 5L HNPC

SHE is a scalar modulation method, which generates the output waveform for the converter simple voltage (in this case, the HB terminals voltage). Therefore, the SHE sets the five-level HB voltage waveform. However, the switching orders within the HB give an additional degree of freedom to be exploited, using Table III to inject/extract current from the dc-link neutral point in order to keep the neutral point balanced.

Therefore, once the SHE angles are calculated, the five-level HB voltage can be generated. When translating the HB voltage into switching states, the only choice that needs to be done is the redundant vector that is desired to be used when $V_{\mathrm{dc}}/2$ or $-V_{\mathrm{dc}}/2$ is applied. $V_{\mathrm{dc}}, -V_{\mathrm{dc}}$ and 0 V levels only have one semiconductor path, as given in Table III. For instance, Fig. 7 shows an example of the first 90º of a 5L PS-SHE6. As it can be appreciated, from 0 V or V_{dc}, it is possible to go to 21 or 10 without any transition state.

Thanks to the SHE properties for HBs, there is no need to modify the output waveform angles in order to regulate the dc-link voltage, which gives a proper elimination of the harmonics. Added to this, always an even number of calculated angles is proposed. Hence, after each 90º of the fundamental period modulation index, output frequency and dc-link neutral point

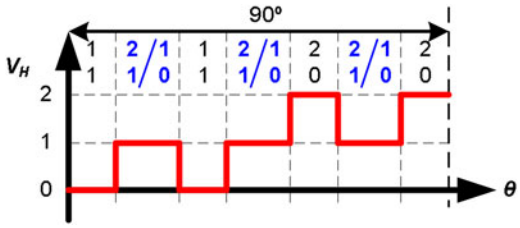

Fig. 7. 5L SHE waveform example expressed in single-phase space vector.

control references are updated without any extra commutation. On the contrary, the dynamic behavior of the system gets slower, which is complete acceptable in some industrial applications such as centrifugal pumps or fans, where this converter topology is used.

Fig. 8 shows an example of HB voltage waveforms using generic SHE. Two cases are illustrated: 5L SHE6 (six calculated angles) and 5L SHE2 (two calculated angles). The way the angles are calculated is independent of this strategy. The update of modulation index, output frequency and dc-link neutral point references are updated each 90º as marked. In blue, redundant vectors are highlighted.

C. DC-Link Neutral-Point Balancing Algorithm Using SHE

One of the main contributions of the paper is oriented to dc-link neutral point control of 5L HNPC, which strategy could be applied to any converter configuration based on HB s with multilevel arms, using any SHE angles, no matter the way they have been calculated. The main question in this topology is which redundant vectors should be selected for a proper dc-link voltage balance.

The proposed dc-link voltage balancing algorithm predicts the current through the dc-link neutral point for the next 90º of the fundamental period. The prediction depends on the output power factor and the used redundant vectors, but is not dependent on the current magnitude. The strategy is based on two main points.

1) The alternation of redundant vectors. Hence, for 0º to 180º, 21/10 vectors are alternated. On the contrary, for 180º to 360º, 01/12 vectors are alternated. Due to this technique, the number of commutations is shared among both HB arms, thus, achieving a better thermal behavior. Added to this, the current in the neutral point is injected/extracted alternatively. For instance, for positive voltage reference, Fig. 8(b) shows the two possible commutation distributions for 90º. Hence, redundant vectors are only placed in even vector numbers of the output waveforms.

   For instance, if positive voltage reference is considered, the first used redundant vector could be 21 or 10. Afterwards, the used vector would be toggled: if 21 was used, the selected one would be 10, and vice versa. Therefore, each 90º the choice is reduced to two possible redundant states combinations (in the first 180º, 21/10/21 . . . or 10/21/10 . . .). Hence, a sign function is defined to know if the current is extracted or injected in the neutral point.

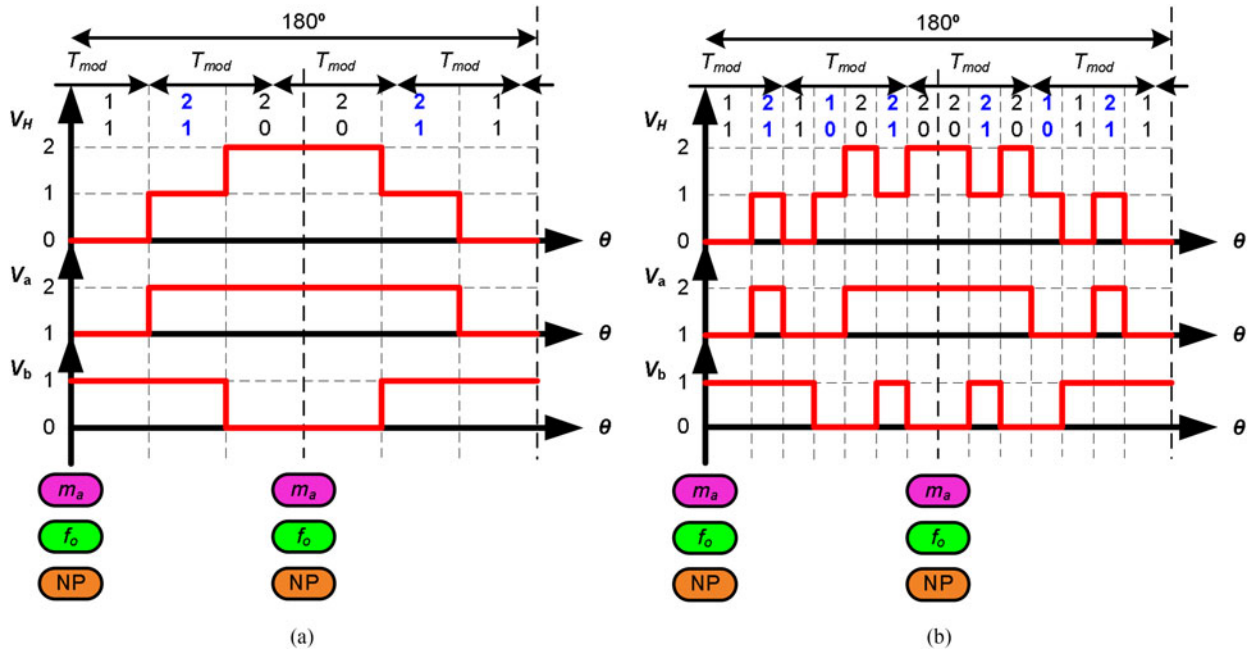

Fig. 8. SHE HB waveforms and modulation index, output frequency and dc-link neutral point references update. v_H is the vector of the HB terminals, v_a and v_b are the vectors of *a* and *b* branches with respect to the neutral point of the bus, respectively. (a) 5L SHE2. (b) 5L SHE6.

For the first 180º of the fundamental period:

$$\begin{cases} \text{If first selected vector 21} \rightarrow \\ s = \text{sign}\ (i_0) = [-1, +1, \ldots]. \\ \text{If first selected vector 10} \rightarrow \\ s = \text{sign}\ (i_0) = [+1, -1, \ldots]. \end{cases} \tag{10}$$

And for the last 180º of the fundamental period:

$$\begin{cases} \text{If first selected vector 12} \rightarrow \\ s = \text{sign}\ (i_0) = [+1, -1, \ldots]. \\ \text{If first selected vector 01} \rightarrow \\ s = \text{sign}\ (i_0) = [-1, +1, \ldots]. \end{cases} \tag{11}$$

2) Knowing there is an alternation in the applied redundant vector, the average dc-link neutral point current for the next 90º of the fundamental harmonic can be predicted ($i_{0,X,\text{ave}}$). For simplicity purposes, only fundamental harmonic is considered in the prediction (further harmonics would need to be considered depending on the scenario)

$$i_{0,\text{X,ave}} = \frac{2}{\pi} \sum_{k=1}^{\frac{N_\alpha}{2}} \int_{\alpha_{(2\cdot k-1)}}^{\alpha_{2\cdot k}} i_{0,\text{X}}\, d\theta = \frac{2}{\pi} \sum_{k=1}^{N_\alpha/2} \int_{\alpha_{(2\cdot k-1)}}^{\alpha_{2\cdot k}} s\,(k) \cdot I_{\text{X}} \cdot \sin\,(\theta - \varphi)\, d\theta \tag{12}$$

where I_X is the amplitude of the load fundamental current and φ is the angle between the HB voltage and current.

As explained, depending on the voltage sign, the number of calculated angles and the voltage next angle gap (from 0º to 180º positive voltage, and from 180º to 360º negative voltage), only two redundant vectors sequence will be available. No matter which the non-redundant vectors are, each of the two available sequences of redundant vectors will always inject the same average neutral point current but with the opposite sign. Therefore, with the proposed method, the following facts can be stated.

1) The number of commutations per branch inside the HB is shared equally each 90º of the fundamental period.
2) Only two voltage (dc-link capacitors voltages) and one current (output phase current, to know the power factor) measurements need to be accomplished.
3) The dc-link neutral point correcting capability is directly dependent on the achieved solution of SHE angles. Moreover, as dc-link capacity is fixed and the angle sets are precalculated, the output current and output frequency mark the amount of charges that can be injected/extracted through the neutral point. Hence, the average dc-link neutral current is fixed by the load current, but current sign can be selected. Therefore, predicting the average current sign through the neutral point using the two possible redundant vectors application is enough to select the optimal. The sign of the average current through the neutral point in the first 90º of the fundamental period can be predicted from (12) as

$$\begin{cases} \text{If first vector is 10 } or \text{ 12} \rightarrow \\ \text{sign}\ (i_{0,\text{ave}}) = \sum_{k=1}^{N_\alpha} (-1)^{\text{trunk}\left(\frac{k}{2}+1\right)} \cos\,(\alpha_k - \varphi) \\ \text{If first vector is 21 } or \text{ 10} \rightarrow \\ \text{sign}\ (i_{0,\text{ave}}) = \sum_{k=1}^{N_\alpha} (-1)^{\text{trunk}\left(\frac{k}{2}+1\right)+1} \cos\,(\alpha_k - \varphi) \end{cases} \tag{13}$$

where φ is the phase between HB voltage and current. This equation is applicable whichever the number of angles is for 5L HNPC converter topology. Furthermore, it is easily extendable to other operating quadrants.

TABLE IV
APPLIED CONSTANTS FOR (14)

	Voltage Angle (θ)	k_{11}	k_{12}	k_{21}	k_{22}	k_{31}	k_{32}	k_{41}	k_{42}	k_{51}	k_{52}	k_{61}	k_{62}
Q1	0º–90º	-1	-1	$+1$	-1	$+1$	-1	-1	-1	-1	-1	$+1$	-1
Q2	90º–180º	-1	$+1$	$+1$	$+1$	$+1$	$+1$	-1	$+1$	-1	$+1$	$+1$	$+1$
Q3	180º–270º	$+1$	-1	-1	-1	-1	-1	$+1$	-1	$+1$	-1	-1	-1
Q4	270º–360º	$+1$	$+1$	-1	$+1$	-1	$+1$	$+1$	$+1$	$+1$	$+1$	-1	$+1$

TABLE V
EXPERIMENTAL TEST BENCH PARAMETERS

Average dc bus voltage (V_{dc}) – DFE 12p	400 V
DC capacitor of half dc bus (C_{X})	3.3 mF
DFE transformer short-circuit impedance	8%
Converter-rated V_{ll} rms voltage	623 V
Converter-rated output rms current	60 A
Output nominal frequency	250 Hz

In the case of the studied SHE6, the result of applying (13) if the first used vector is 10 or 12

$$\begin{aligned}\operatorname{sign}\left(i_{0,\mathrm{ave}}\right) = k_{11}\cdot\cos\left(\alpha_1 + k_{12}\cdot\varphi\right) + k_{21}\\ \cdot\cos\left(\alpha_2 + \mathrm{k}_{22}\cdot\varphi\right) + k_{31}\\ \cdot\cos\left(\alpha_3 + k_{32}\cdot\varphi\right) + k_{41}\\ \cdot\cos\left(\alpha_4 + k_{42}\cdot\varphi\right) + k_{51}\\ \cdot\cos\left(\alpha_5 + k_{52}\cdot\varphi\right) + k_{61}\\ \cdot\cos\left(\alpha_6 + k_{62}\cdot\varphi\right)\end{aligned} \tag{14}$$

where the values of the constants are given in Table IV.

Once the average neutral point current sign is predicted, based on dc-link capacitors voltages ($V_{C1} - V_{C2}$), the more convenient first redundant vector is selected, thus, the switching patter for the next 90º is fixed. A hysteresis band is proposed when changing the direction the neutral point is wanted to be corrected, so as to avoid possible measurement uncertainties.

IV. SIMULATION AND EXPERIMENTAL RESULTS

With the aim of demonstrating the operability of the ideas proposed in this paper, a downscaled platform is built in the Medium Voltage Laboratory of Ingeteam Power Technology, S.A. (Zamudio, Spain). Two main points need to be proven:

1) the suitability of PS-SHE against ML-SHE;
2) the optimal operation of whole proposed solution: PS-SHE + dc-link neutral point regulation strategy in a 5L HNPC converter.

Therefore, with this purpose, the test bench shown in Fig. 9 is built. The electrical scheme is the one shown in Fig. 5, feeding each dc-link with a 3×12 DFE, with three isolated transformers. Although Fig. 9(a) shows one single-phase 5L HNPC, a whole three-phase 5L HNPC is built. The principal characteristics of the test bench are summarized in Table V.

As it can be observed in Table V, the test bench is prepared to work up to 250 Hz of output frequency. In order to reach this output frequency, different modulation techniques can be applied: different SHE solutions and PWM are implemented [8]. Adjustable inductor loads are used, which can go from 3.2 to 15 mH; the values of the loads are changed off-line depending on the experiment.

TABLE VI
EXPERIMENTAL CIRCUIT PARAMETERS FOR 5L PS-SHE6 AND 5L ML-SHE6 COMPARISON

Modulation index	0.538
Load inductance experimental (L_{load})	15 mH

The two 5L SHE6 (5L PS-SHE6 and 5L ML-SHE6) alternatives and the dc-link neutral point control are implemented. Additionally, 5L PS-SHE2 is also implemented. The calculations are carried out into a DSP, which sends vectors and times to three FPGAs. Each HB has one associated FPGA, which sends the switching orders to the drivers and helps to the measurements of needed voltages and currents by means of transducers. As explained, two voltage measurements are needed, as well as, one output current measurement per HB.

A. PS-SHE6 and ML-SHE6 Angles Comparison

The angles employed for 5L SHE6 modulation, are shown in Figs. 2 and 4(b), for ML-SHE6 and PS-SHE6, respectively. In these graphs, $m_a = 1$ means that the converter reaches 623 Vrms in the line-to-line voltage. However, as the number of angles and levels increases, the maximum achievable modulation index decreases. Due to this reason, none of the two studied solutions reaches $m_a = 1$ point.

In order to compare ML-SHE with the proposed PS-SHE, $m_a{}^{\circ} = 0.538$ point is selected for both angle solutions, for 50 Hz output frequency (see Table VI). This point is chosen in order to show how with very different output waveforms, both angle solutions reach the same fundamental voltage value. The HB voltages obtained are shown in Fig. 10. Added to this, Table VII shows the values of the lower harmonics that can be significant in line-to-line voltages; for instance, zero sequence harmonics appear in $\mathrm{X} = \{\mathrm{R}, \mathrm{S}, \mathrm{T}\}$ phase output terminal voltage ($V_{\mathrm{X,ab}}$), but will disappear in line-to-line voltages, as it can be appreciated in the load current. Added to this, the load inductance is set to $L_{\mathrm{load}} = 15\mathrm{mH}$.

The HB voltage and output current THDs are also calculated, which are defined as

$$\mathrm{THDv} = \frac{\sqrt{\sum_{h=2}^{\infty}\left(V_h\right)^2}}{V_1} \tag{15}$$

$$\mathrm{THDi} = \frac{\sqrt{\sum_{h=2}^{\infty}\left(I_h\right)^2}}{I_1} \tag{16}$$

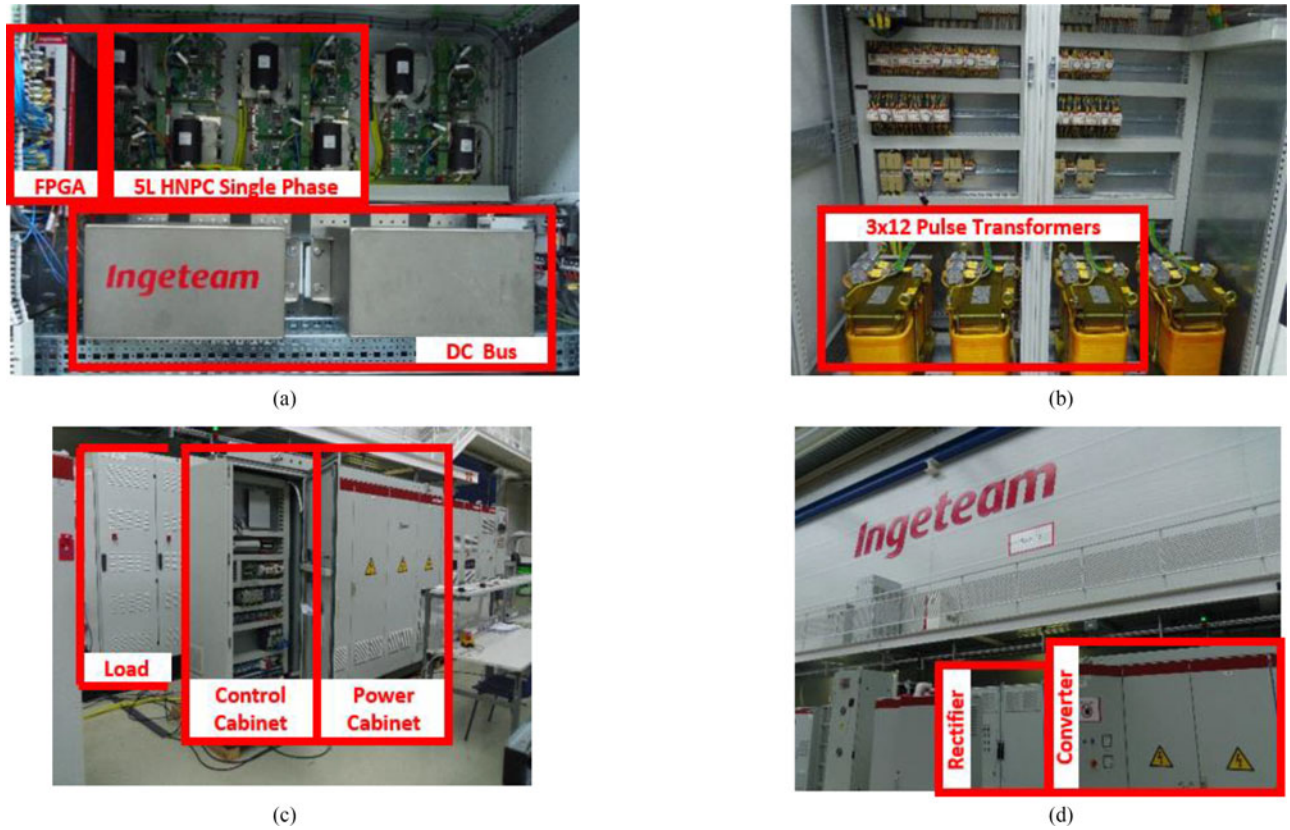

Fig. 9. Downscaled test bench layout.

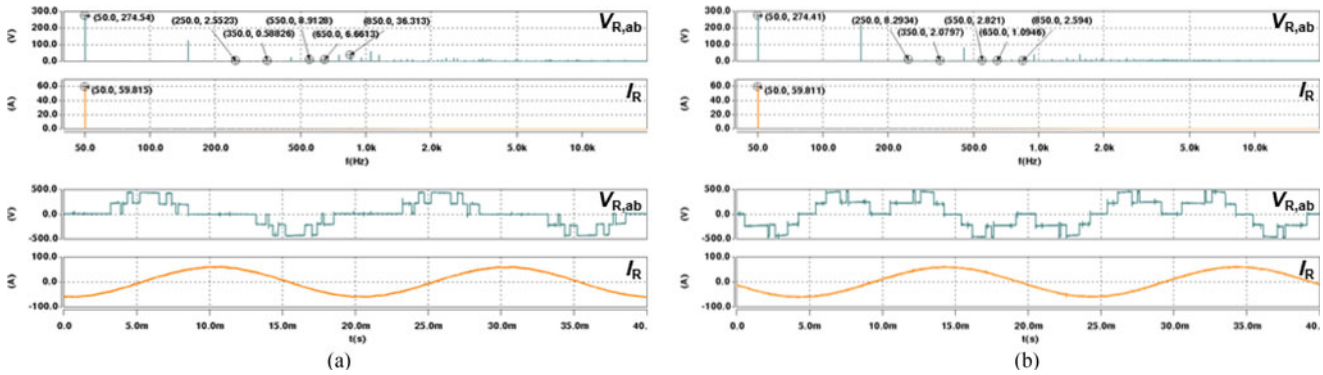

Fig. 10. HB voltage and current experimental spectra and waveforms. (a) PS-SHE6. (b) ML-SHE6. From top to bottom: HB terminals voltage (cyan) and output current (orange).

TABLE VII
HB OUTPUT VOLTAGE HARMONICS SIMULATION BEHAVIOR

	n-Harmonic Value (V)						THDv	THDi
	1	5	7	11	13	17		
5L PS-SHE6 (see Fig. 4(b))	274.54	2.5523	0.58826	8.9128	6.6613	36.313	59.838%	2.869%
5L ML-SHE6 (see Fig. 2)	274.41	0.2934	2.0797	2.821	1.0946	2.594	91.449%	3.7506%

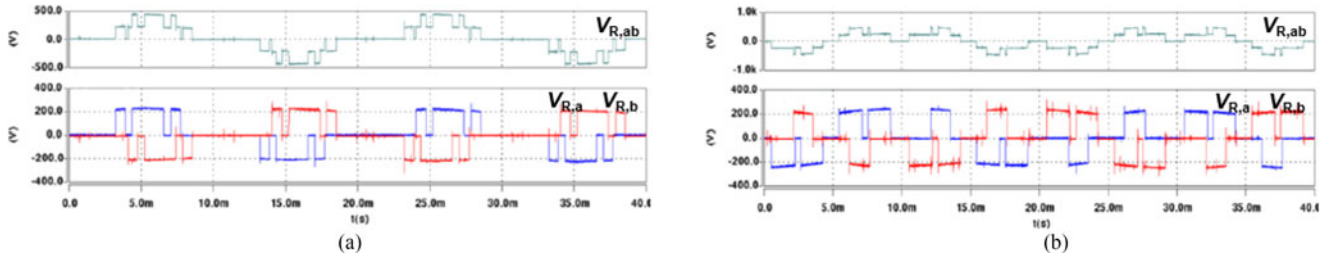

Fig. 11. HB voltages waveforms. (a) PS-SHE6. (b) ML-SHE6. From top to bottom: HB terminals voltage (cyan), *a* arm voltage (blue) and *b* arm voltage (red).

where V_h and I_h are the h order voltage and current harmonics, respectively.

The following points can be concluded comparing these two SHE alternatives:

1) The elimination of low harmonics achieved with 5L ML-SHE6 is better than using 5L PS-SHE6.
2) The THD achieved using 5L PS-SHE6 is better than the one obtained by means of 5L ML-SHE6 (both in voltage and current). Considering $V_{\mathrm{X,ab}}$ THD, zero sequence harmonics are taken into account. Creating a low zero sequence voltage is a good point for a modulation technique. This is why THD of HB voltage is considered. Regarding the line-to-line voltage waveform, output current can give a comparable value of the output line-to-line voltage quality; this time, 5L PS-SHE6 is more competitive again than the 5L ML-SHE6.

Although ML-SHE eliminates lower harmonics, PS-SHE achieves better THD results, since the minimization of the harmonics is repeated in multiple harmonics of the first mitigated harmonic couple (as shown in (7) and given in Table I). Therefore, even if non-eliminated and non-minimized harmonics are not controlled, 5L PS-SHE6 achieves better behavior in THD (both, in voltage and current).

Although this is an operating point example, it demonstrates that 5L PS-SHE6 is a competitive alternative to 5L ML-SHE6. Furthermore, as main potential, continuous angle sets solution is attained, which gives better dynamic behavior to the system.

To finish with the comparison, Fig. 11 shows HB voltages using both SHE solutions and the distribution of the voltages in each arm inside the HB. As stated before, the commutations are shared among both branches, whichever the utilized angles solution is. This share is given thanks to the dc-link neutral point algorithm proposed.

B. DC-Link Neutral Point Control

As it is mentioned in the previous section, the proposed PS-SHE is an interesting SHE alternative. In this sub-section, the capability of regulating the dc-link neutral point is demonstrated. With that purpose, the dc-link voltages evolution of 5L PS-SHE2 and 5L PS-SHE6 is analyzed. The hysteresis band applied to the dc-link neutral point regulator is fixed to 5 V. This means that if "$|V_{C1} - V_{C2}| > 5$", the dc-link neutral point voltage is corrected in the other direction.

In the proposed scenario, as different number of SHE angles are analyzed, each of them is studied with different output frequency and load current conditions. This is done so, in order to emulate real operation, where less number of angles will be used for higher output current or/and frequency, thus, not reaching the thermal limit of the semiconductors. The use of each modulation technique is carried out according to [8].

TABLE VIII
EXPERIMENTAL CIRCUIT PARAMETERS FOR 5L PS-SHE2

Output frequency	200 Hz
Modulation index	0.796
Load inductance experimental (L_{load})	3.2 mH

TABLE IX
EXPERIMENTAL CIRCUIT PARAMETERS FOR 5L PS-SHE6

Output frequency	100 Hz
Modulation index	0.398
Load inductance experimental (L_{load})	3.2 mH

For 5L PS-SHE2, the evaluated operating point is presented in Table VIII and the obtained results in Fig. 12.

The following points can be concluded from Fig. 12:

1) the dc-link neutral point regulation is achieved properly;
2) a small offset in the measurement of the voltages can be appreciated;
3) the hysteresis band of ± 5 V gives a 10 V ripple of capacitor filtered voltages subtraction. It can be noted, analyzing last graph of Fig. 12(b), how after 12 ms, the red pulse goes after the blue pulse. This means that the neutral point controller wants to correct the $(V_{C1} - V_{C2})$ in the other direction.

For 5L PS-SHE6, the evaluated operating point is presented in Table IX and the obtained results in Fig. 13. From this graph, the following points can be concluded:

1) the dc-link neutral point regulation is achieved properly, in this case, as the redundant vectors application time is very small, the capacitors voltages change much more slowly than in the case of PS-SHE2 angles;
2) a clear dc-link correcting trend change can be again appreciated around 12 ms.

In these two examples, a proper regulation of the dc-link voltages can be appreciated, in different modulation indices and output frequencies. These two examples demonstrate the operability and suitability of the proposed dc-link strategy. Added

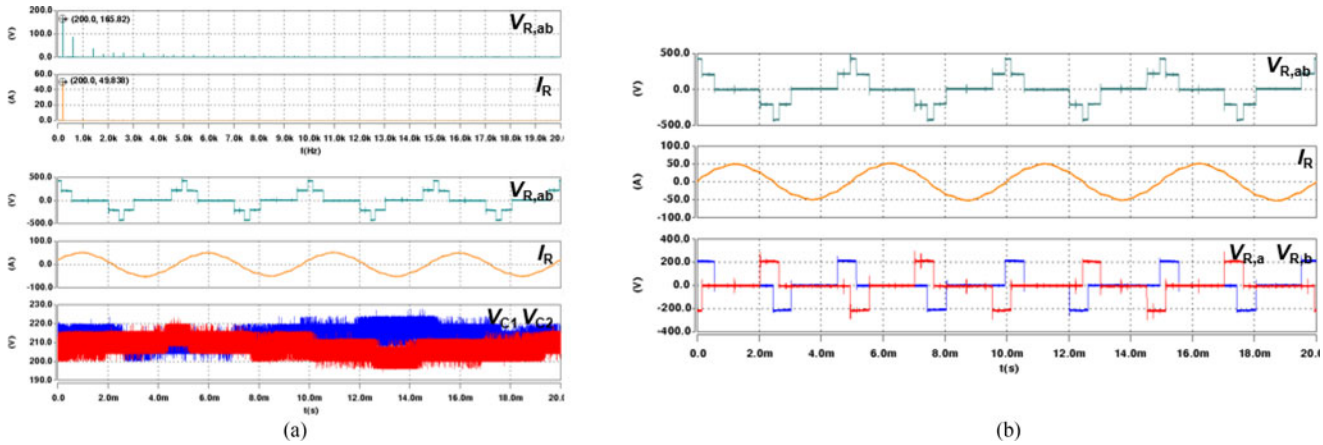

Fig. 12. HB voltages waveforms applying 5L PS-SHE2 angles. (a) From top to bottom: HB terminals voltage (cyan), output current (orange), and capacitors voltages (red and blue). (b) From top to bottom: HB terminals voltage (cyan), output current (orange), and HB arms voltages (red and blue).

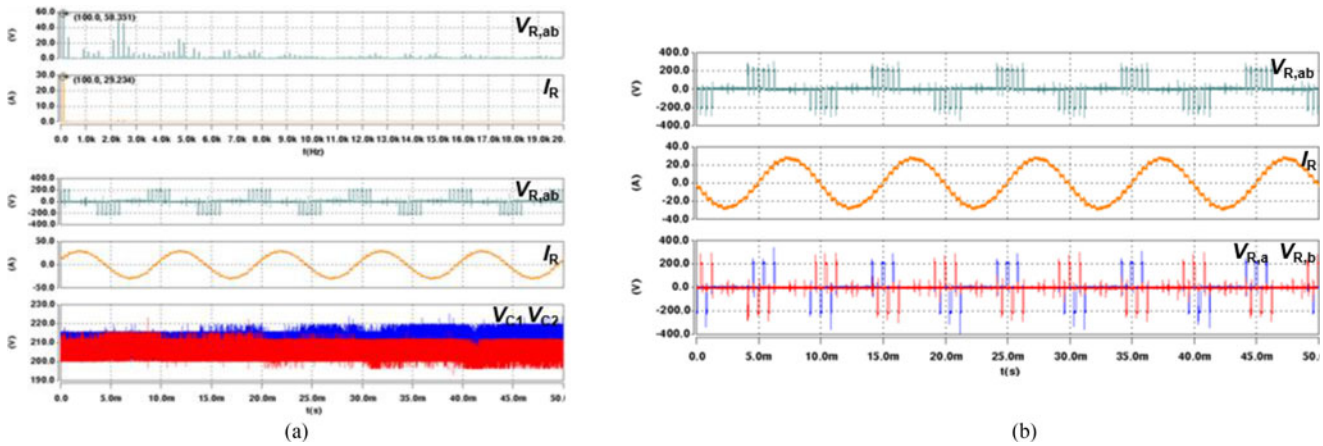

Fig. 13. HB voltages waveforms applying PS-SHE6 angles. (a) From top to bottom: HB terminals voltage (cyan), output current (orange), and capacitors voltages (red and blue). (b) From top to bottom: HB terminals voltage (cyan), output current (orange), and HB arms voltages (red and blue).

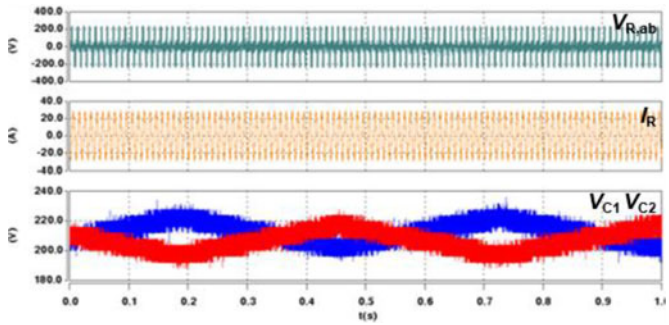

Fig. 14. HB voltages waveforms applying PS-SHE6 angles with 20 V of dc-link hysteresis. From top to bottom: HB terminals voltage (cyan), output current (orange), and capacitors voltages (red and blue).

to this, the spectra of the voltages in Figs. 12(a) and 13(a) show how PS-SHE ensures the elimination/minimization of the mentioned harmonics. Added to this, the share of equal number of commutations per HB arms can be appreciated, which ensures a good thermal share among different semiconductors in the converter.

Finally, Fig. 14 shows 5L PS-SHE6 angles with the conditions specified in Table IX, but having 20 V of hysteresis value for the neutral point regulation. It can be clearly appreciated how the voltage oscillation of the capacitor is augmented.

All these results demonstrate the suitability and effectiveness of the proposed dc-link neutral point regulation method, in combination with PS-SHE solutions.

V. Conclusion

This paper presents the Phase Shifted SHE (PS-SHE), which is based on the calculation of 3L SHE angles, increasing the number of levels by means of a phase shifts; each phase shift will add minimization of undesired harmonics. The complexity of solving 3L SHE equations compared with SHE equations of higher levels is dramatically reduced. Thanks to this, a continuous solution of SHE angle sets is achieved for the whole modulation index range. This makes PS-SHE a competitive overall solution for variable speed inverters, which have to deal with very different modulation index ranges. This calculation method can be used for single-phase and three-phase converters.

Added to this, a dc-link capacitors voltage balancing strategy is proposed, for HB-based converters with multilevel arms and

SHE modulation technique. This method allows to have controlled dc-link voltages oscillation by means of a prediction of the neutral point current through the neutral point. Furthermore, dc-link neutral point is controlled without the need of any additional commutation and completely sharing the commutations among the HB arms, which achieves an optimal thermal balance in the converter.

The combination of both strategies (PS-SHE angle sets calculation and dc-link neutral point control) is experimentally served by means of a downscaled test bench of a three-phase 5L HNPC converter. However, both presented strategies can be easily extrapolated to converters with higher number of levels.

REFERENCES

[1] S. Kouro, M. Malinowski, K. Gopakumar, J. Pou, L. G. Franquelo, Bin Wu, J. Rodriguez, M. A. Perez, and J. I. Leon, "Recent advances and industrial applications of multilevel converters," *IEEE Trans. Ind. Electron.*, vol. 57, no. 8, pp. 2553–2580, Aug. 2010.

[2] L. M. Tolbert, F. Zheng Peng, and T. G. Habetler, "Multilevel converters for large electric drives," *IEEE Trans. Ind. Appl.*, vol. 35, no. 1, pp. 36–44, Feb. 1999.

[3] A. Sanchez-Ruiz, M. Mazuela, S. Alvarez, G. Abad, and I. Baraia, "Medium voltage—High power converter topologies comparison procedure, for a 6.6 kV drive application using 4.5 kV IGBT modules," *IEEE Trans. Ind. Electron.*, vol. 59, no. 3, pp. 1462–1476, Mar. 2012.

[4] S. Kouro, J. Rodriguez, Bin Wu, S. Bernet, and M. Perez, "Powering the future of industry: High-power adjustable speed drive topologies," *IEEE Ind. Appl. Mag.*, vol. 18, no. 4, pp. 26–39, Aug. 2012.

[5] J. A. Barrena, L. Marroyo, M. A. R. Vidal, and J. R. T. Apraiz, "Individual voltage balancing strategy for PWM cascaded H-bridge converter-based STATCOM," *IEEE Trans. Ind. Electron.*, vol. 55, no. 1, pp. 21–29, Jan. 2008.

[6] J. Chivite-Zabalza, M. A. Rodriguez Vidal, P. Izurza-Moreno, G. Calvo, and D. Madariaga, "A large-power voltage source converter for FACTS applications combining three-level neutral-point-clamped power electronic building blocks," *IEEE Trans. Ind. Electron.*, vol. 60, no. 11, pp. 4759–4772, Nov. 2013.

[7] M. Zabaleta, E. Burguete, D. Madariaga, I. Zubimendi, M. Zubiaga, and I. Larrazabal, "LCL grid filter design of a multimegawatt medium-voltage converter for offshore wind turbine using SHEPWM modulation," *IEEE Trans. Power Electron.*, vol. 31, no. 3, pp. 1993–2001, Mar. 2016.

[8] A. Sanchez-Ruiz, G. Abad, S. Alvarez, and L. M. Tolbert, "Modulation selection procedure applied to a high-power adjustable high-speed drive," in *Proc. 2013 15th Eur. Conf. Power Electron. Appl.*, 2013, pp. 1–10.

[9] J. Holtz, "Pulsewidth modulation for electronic power conversion," *Proc. IEEE*, vol. 82, no. 8, pp. 1194–1214, Aug. 1994.

[10] S. Busquets-Monge, S. Alepuz, J. Rocabert, and J. Bordonau, "Pulsewidth modulations for the comprehensive capacitor voltage balance of -level three-leg diode-clamped converters," *IEEE Trans. Power Electron.*, vol. 24, no. 5, pp. 1364–1375, May 2009.

[11] N. Celanovic and D. Boroyevich, "A fast space-vector modulation algorithm for multilevel three-phase converters," *IEEE Trans. Ind. Appl.*, vol. 37, no. 2, pp. 637–641, Apr. 2001.

[12] D. Ahmadi, K. Zou, C. Li, Y. Huang, and J. Wang, "A universal selective harmonic elimination method for high-power inverters," *IEEE Trans. Power Electron.*, vol. 26, no. 10, pp. 2743–2752, Oct. 2011.

[13] G. Konstantinou, V. G. Agelidis, and J. Pou, "Theoretical considerations for single-phase interleaved converters operated with SHE-PWM," *IEEE Trans. Power Electron.*, vol. 29, no. 10, pp. 5124–5128, Oct. 2014.

[14] M. S. A. Dahidah, G. Konstantinou, and V. G. Agelidis, "A review of multilevel selective harmonic elimination PWM: Formulations, solving algorithms, implementation and applications," *IEEE Trans. Power Electron.*, vol. 30, no. 8, pp. 4091–4106, Aug. 2015.

[15] J. Napoles, J. I. Leon, R. Portillo, L. G. Franquelo, and M. A. Aguirre, "Selective harmonic mitigation technique for high-power converters," *IEEE Trans. Ind. Electron.*, vol. 57, no. 7, pp. 2315–2323, Jul. 2010.

[16] A. K. Rathore, J. Holtz, and T. Boller, "Synchronous optimal pulsewidth modulation for low-switching-frequency control of medium-voltage multilevel inverters," *IEEE Trans. Ind. Electron.*, vol. 57, no. 7, pp. 2374–2381, Jul. 2010.

[17] W. Fei, X. Ruan, and B. Wu, "A generalized formulation of quarter-wave symmetry SHE-PWM problems for multilevel inverters," *IEEE Trans. Power Electron.*, vol. 24, no. 7, pp. 1758–1766, Jul. 2009.

[18] K. Yang, Q. Zhang, J. Zhang, R. Yuan, Q. Guan, W. Yu, and J. Wang, "Unified selective harmonic elimination for multilevel converter," *IEEE Trans. Power Electron.*, vol. PP, no. 99, pp. 1–1, 2016.

[19] J. Pou, R. Pindado, D. Boroyevich, and P. Rodriguez, "Limits of the neutral-point balance in back-to-back-connected three-level converters," *IEEE Trans. Power Electron.*, vol. 19, no. 3, pp. 722–731, May 2004.

[20] M. Saeedifard, R. Iravani, and J. Pou, "Analysis and control of DC-capacitor-voltage-drift phenomenon of a passive front-end five-level converter," *IEEE Trans. Ind. Electron.*, vol. 54, no. 6, pp. 3255–3266, Dec. 2007.

[21] S. R. Pulikanti, M. S. A. Dahidah, and V. G. Agelidis, "Voltage balancing control of three-level active NPC converter using SHE-PWM," *IEEE Trans. Power Deliv.*, vol. 26, no. 1, pp. 258–267, Jan. 2011.

[22] S. R. Pulikanti, G. Konstantinou, and V. G. Agelidis, "Hybrid seven-level cascaded active neutral-point-clamped-based multilevel converter under SHE-PWM," *IEEE Trans. Ind. Electron.*, vol. 60, no. 11, pp. 4794–4804, Nov. 2013.

[23] J. Shen, S. Schröder, B. Qu, Y. Zhang, K. Chen, F. Zhang, and R. Zhang, "Modulation schemes for a 30-MVA IGCT converter using NPC H-bridges," *IEEE Trans. Ind. Appl.*, vol. 51, no. 5, pp. 4028–4040, Oct. 2015.

[24] I. Etxeberria-Otadui, A. Lopez-de-Heredia, J. San-Sebastian, H. Gaztanaga, U. Viscarret, and M. Caballero, "Analysis of a H-NPC topology for an AC traction front-end converter," in *Proc. 13th Power Electron. Motion Control Conf.*, 2008, pp. 1555–1561.

[25] C. A. Rojas, S. Kouro, D. Edwards, Bin Wu, and S. Rivera, "Five-level H-bridge NPC central photovoltaic inverter with open-end winding grid connection," in *Proc. 2014 40th Annu. Conf. IEEE Ind. Electron. Soc.*, 2014, pp. 4622–4627.

[26] J. Shen, S. Schröder, B. Qu, Y. Zhang, K. Chen, F. Zhang, Y. Li, Y. Liu, P. Dai, and R. Zhang, "A high-performance 2×27 MVA machine test bench based on multilevel IGCT converters," *IEEE Trans. Ind. Appl.*, vol. 51, no. 5, pp. 3877–3889, Oct. 2015.

[27] D. G. Holmes and B. P. McGrath, "Opportunities for harmonic cancellation with carrier-based PWM for a two-level and multilevel cascaded inverters," *IEEE Trans. Ind. Appl.*, vol. 37, no. 2, pp. 574–582, Apr. 2001.

[28] M. S. A. Dahidah and V. G. Agelidis, "Selective harmonic elimination PWM control for cascaded multilevel voltage source converters: A generalized formula," *IEEE Trans. Power Electron.*, vol. 23, no. 4, pp. 1620–1630, Jul. 2008.

[29] V. G. Agelidis, A. I. Balouktsis, and C. Cossar, "On attaining the multiple solutions of selective harmonic elimination PWM three-level waveforms through function minimization," *IEEE Trans. Ind. Electron.*, vol. 55, no. 3, pp. 996–1004, Mar. 2008.

[30] Y. Yang, K. Zhou, H. Wang, F. Blaabjerg, D. Wang, and B. Zhang, "Frequency adaptive selective harmonic control for grid-connected inverters," *IEEE Trans. Power Electron.*, vol. 30, no. 7, pp. 3912–3924, Jul. 2015.

[31] A. Laka, J. A. Barrena, J. Chivite-Zabalza, and M. A. Rodriguez, "Analysis and improved operation of a PEBB-based voltage-source converter for FACTS applications," *IEEE Trans. Power Deliv.*, vol. 28, no. 3, pp. 1330–1338, Jul. 2013.

Alain Sanchez-Ruiz (S'10–M'15) was born in Barakaldo, Spain, in 1985. He received the B.Sc. degree in electronics engineering, the M.Sc. degree in automatics and industrial electronics, and the Ph.D. degree in electrical engineering from the University of Mondragon, Mondragon, Spain, in 2006, 2009, and 2014, respectively.

He joined Ingeteam Power Technology, Zamudio, Spain, in May 2014, where he is currently an R&D Engineer in the Industrial and Marine Drives Business Unit. His current research interests include modeling, modulation and control of power converters, multilevel topologies, advanced modulation techniques and high-power motor drives.

Gonzalo Abad (M'07) received the B.Sc. degree in electrical engineering from the University of Mondragon, Mondragon, Spain, in 2000, the M.Sc. degree in advanced control from the University of Manchester, Manchester, UK, in 2001, and the Ph.D. degree in electrical engineering from the University of Mondragon, in 2008.

He joined the Electronics Department of the University of Mondragon in 2001, where he is currently an Associate Professor. His current research interests include renewable energies, power conversion, and motor drives. He has authored or coauthored several papers in the areas of wind power generation, multilevel power converters and direct torque control of ac drives. He has participated in different industrial projects related to these fields.

Ivan Echeverria was born in Pamplona, Spain, in 1977. He received the M.S. degree in industrial engineering from the Public University of Navarre, Pamplona, Spain, in 2002.

He joined Ingeteam Power Technology, Zamudio, Spain, in 2002, where he is currently a Product Engineer in Medium Voltage Drives for Industrial and Marine Drives Business Unit. His current research interests include the design and development of high-power/medium-voltage and high efficiency power converters.

Iñigo Torre was born in Bilbao, Spain, in 1977. He received the M.Sc. degree in electrical engineering from the University of Mondragon, Mondragon, Spain, in 2001.

From 2001 to 2008, he was an R&D Engineer for Ingeteam Power Technology, Zamudio, Spain. Since 2009, he has been a Control Engineer in the Industrial & Marine Drives Business Unit of Ingeteam Power Technology, developing and testing control algorithms for the frequency converters.

Iñigo Atutxa was born in Zeanuri, Spain, in 1981. He received the B.Sc. and M.Sc. degrees in electrical engineering from Mondragon University, Mondragon, Spain, in 2001 and 2004, respectively.

From 2004 to 2012, he was with Ingeteam Power Technology, Zamudio, Spain, as an R&D Engineer, where he was engaged in projects related to the design and development of medium-voltage and low-voltage variable-speed drives, for several different applications located on the industrial, marine, traction, energy, and mining markets. Since 2012, he has been with Ingeteam Power Technology as a Technical Director for Industrial and Marine Drives Business Unit. He has contributed in more than ten research and technical papers, books, and patents in the fields of variable-speed drives and power electronics.